Cluster Morphology-Polymer Dynamics Correlations in Sulfonated Polystyrene Melts: Computational Study

Anupriya Agrawal,[1,2] Dvora Perahia,[1] and Gary S. Grest[3]
[1]Department of Chemistry, Clemson University, Clemson, South Carolina 29634, USA
[2]Department of Mechanical Engineering and Materials Science, Washington University in St. Louis, St. Louis, Missouri 63130, USA
[3]Sandia National Laboratories, Albuquerque, New Mexico 87185, USA

(Received 4 December 2015; revised manuscript received 19 February 2016; published 11 April 2016)

Reaching exceptionally long times up to 500 ns in equilibrium and nonequilibrium molecular dynamics simulations studies, we have attained a fundamental molecular understanding of the correlation of ionomer clusters structure and multiscale dynamics, providing new insight into one critical, long-standing challenge in ionic polymer physics. The cluster structure in melts of sulfonated polystyrene with Na^+ and Mg^{2+} counterions are resolved and correlated with the dynamics on multiple length and time scales extracted from measurements of the dynamic structure factor and shear rheology. We find that as the morphology of the ionic clusters changes from ladderlike for Na^+ to disordered structures for Mg^{2+}, the dynamic structure factor is affected on the length scale corresponding to the ionic clusters. Rheology studies show that the viscosity for Mg^{2+} melts is higher than for Na^+ ones for all shear rates, which is well correlated with the larger ionic clusters' size for the Mg^{2+} melts.

DOI: 10.1103/PhysRevLett.116.158001

Ionomers are in the core of many applications including ion exchange membranes, water separation, sensors, and others [1–3]. Their mechanical and viscoelastic response as well as their transport characteristics strongly depend on the number of ionizable groups on the polymer chain. These ionizable groups segregate into long-lived clusters independent of anions and cations present [2]. Examples include ionomers containing sulfonates [4,5], carbonates [6,7], or phosphonates [8,9], which all form ionic domains with various morphologies. As the ionic aggregates serve as physical cross-linkers, the morphology of these assemblies and their internal dynamics is one critical component in determining the overall properties of ionomers. While the formation of clusters in ionomers has been observed, the factors that control their shape and size remain an open question despite immense efforts. Being able to probe computationally long times commensurate with the actual segmental dynamics time scales in ionomers, now possible with new computational tools, this study provides a new fundamental insight into the factors that impact the dynamics of ionic polymers.

The size and shape of the ionic cluster result from a balance between electrostatic interactions, size of the ionic groups, and counterions as well as the behavior of the polymeric chains that is determined by the dielectric constant of the environment [10]. The counterion is one important entity that is not only responsible for electrical neutrality but also impacts the cluster formation and their size in ionic polymers [11]. Using equilibrium and nonequilibrium molecular dynamics (MD) simulations, we obtained a molecular level insight into the effects of the counterions on the size and shape of the ionic clusters in one model polymer, polystyrene sulfonate (PSS), and directly correlated these characteristics with dynamics of the polymers for the first time on multiple length scales through measuring the dynamic structure factor $S(q, t)$ and the macroscopic shear rheology of the melts.

Specifically we have investigated melts of PSS fully neutralized with two counterions Na^+ and Mg^{2+} (PSS/Na^+ and PSS/Mg^{2+}), correlating cluster morphology with multiscale dynamics. This polymer has been extensively studied, offering a wealth of knowledge to compare with and validate the choice of the force fields. We show a direct correlation between the polymer dynamics as the morphology of the ionic clusters changes from ladderlike with extended ribbons that consist of SO_3^- and Na^+ pairs for PSS/Na^+ melts to elongated, disordered structures for PSS/Mg^{2+}.

The significance of ionic clusters for both transport and stability of ionomers has led to numerous studies of the size and shape of clusters and their impact on rheology of the polymers. While a variety of different clusters were observed, one universal conclusion has been that the ionic groups impede the dynamics of the polymers. However, there is hardly any explanation for the dramatic effects on mobility induced by a small fraction of ionizable groups. Kirkmeyer *et al.* [12], for example, showed that the cluster morphology changes from spherical to vesicular with the change in neutralization levels of PSS. Zhou *et al.* [5] reported that the size of the ionic aggregates increased with increasing cation radius independent of the cation valency; however, the cation concentrations of the ionic aggregates are higher for monovalent cations than for divalent cations. In contrast, Castagna *et al.* [13] found that ionic aggregate

size is independent of sulfonation fraction, degree of neutralization, and ionic radius of cations. They observed one broad segmental relaxation process for monovalent cations and two distinct segmental relaxation processes for divalent cations, in Na^+, Cs^+, and Zn^{2+} neutralized PSS melts. The impact on dynamics is slightly less explored where Weiss and Zhao [14] reported that increasing sulfonation and decreasing cation size of monovalent alkali metal cations result in higher melt viscosity in PSS melts. Ling *et al.* [15] have shown that the rheology and response to elongation flow of PSS are similar to that of highly entangled polymers. Further, Qiao and Weiss [16] have shown that nonlinear rheological behavior of PSS melts significantly differed from entangled polystyrene melts. These comprehensive experimental studies have clearly demonstrated that the cations impact the size and shape of the clusters and often the mobility of the polymers.

Further insight was obtained from MD simulations for a variety of ionomer melts [10,17,18] and aqueous polyelectrolyte solutions [19,20]. Using a coarse-grained polymer model Hall *et al.* [21] have shown that polymer architecture impacts the fluidity of the ionic aggregates. Melt studies using atomistic simulation by Bolintineanu *et al.* [17] revealed that in ionomers with precisely spaced ionizable groups, for Na^+, Li^+, Zn^{2+}, and Cs^{2+} counterions, aggregate with morphologies ranging from small spherical clusters and stringlike chains to large percolating network exists. Buitrago *et al.* [18] have shown that the calculated structure factors of these ionomer melts are in agreement with x-ray studies, further validating the complex structures of the ionic clusters and the ability to probe these types of polymers by MD studies. Both experimental and simulation studies have demonstrated that electrostatic interactions impact cluster morphology in a wide range of ionomers. Using atomistic MD simulations, Agrawal *et al.* have shown that morphological transformation from ladderlike clusters to globular assemblies in PSS/Na^+ melts can be induced by increasing the dielectric constant of the media. They have clearly demonstrated that the decrease in electrostatic interaction impacts the cluster morphology, and in turn enhances significantly the mobility of the ionomers [10]. These studies pointed to correlations of cluster morphology and viscoelastic behavior, though the direct effects on the ionomers' dynamics remains unresolved. Here, using all-atom MD simulations of PSS melt with Na^+ or Mg^{2+} counterions, we probed cluster morphology and their impact on segmental dynamics and viscosity on multiple length scales.

Sulfonated polystyrene is modeled using the All Atom Optimized Potential for Liquid Simulations (OPLS-AA) force field by Jorgensen *et al.* [22,23]. Additional parameters for sulfonate SO_3^- group are given in Refs. [24–26]. The nonbonded interaction is a sum of standard 12-6 Lennard-Jones (LJ) and electrostatic potentials. Nonbonded interactions are calculated between all atom pairs of different molecules. In addition, all pairs on the same molecule separated by three or more bonds are included in nonbonded interactions, though the interaction is reduced by a factor of 1/2 for atoms separated by three bonds. The attractive (r^{-6}) dispersion term in the LJ interaction as well as the electrostatic interactions were calculated using the particle-particle particle-mesh (PPPM) algorithm [27]. As a result, the LJ interaction becomes a fully long-range potential. Interactions closer than 1.2 nm are calculated in real space; those outside this range are calculated in reciprocal Fourier space with precision of 10^{-4}. The repulsive (r^{-12}) LJ interaction was truncated at 1.2 nm. The simulations were performed using the Large Atomic Molecular Massive Parallel Simulator (LAMMPS) molecular dynamics code [28]. The Newton equations of motion were integrated using a velocity-Verlet algorithm with each atom coupled weakly to a Langevin thermostat with a damping constant of 100 fs to maintain a constant temperature. The reference system propagator algorithm (RESPA) with multi-time-scale integrator [29,30] was used to accelerate the simulation. A time step of 1.0 fs for the bond, angle, dihedral, van der Waals interactions, and direct interactions part of the electrostatic interactions and a time step 4.0 fs for long-range electrostatic interactions were used in all of the simulations.

All of the results presented here are for randomly sulfonated atactic polystyrene chains of 80 monomers (8320 g/mol) with sulfonation levels 0%, 5%, and 10% with either Na^+ or Mg^{2+} counterions. The 0%, 5%, and 10% systems contained 160, 312, and 320 chains, respectively. Periodic boundary conditions were used in all simulations. These systems were first equilibrated at 600 K at constant pressure of 1 atm using the Nosé-Hoover thermostat and barostat. The resulting densities of the melts at 1 atm at 600 K are 0.903 and 0.95 g/cm^3 for sulfonation 5% and 10%, respectively, for PSS/Na^+ and 0.898 g/cm^3 for 5% sulfonation PSS/Mg^{2+}, compared to 0.84 g/cm^3 at 600 K and 0.905 g/cm^3 at 500 K for the neat polystyrene (PS). Each of these systems then was run at constant volume for 300–500 ns. To measure the viscosity, we integrated the SLLOD (which adopts the transpose of the qp-DOLLS tensor) equations of motion [31,32] at strain rates of $\dot{\gamma} = 10^7$ to 10^{10}/s with a damping constant of 1 ps. The shear viscosity is calculated using $\eta = -\langle P_{xz}\rangle/\dot{\gamma}$, where $\langle P_{xz}\rangle$ is the xz component of the pressure tensor along the flow and gradient directions, respectively. In LAMMPS, the PPPM algorithm has been implemented for nonrectangular simulation cells only for the Coulomb interactions; therefore, the LJ potential was truncated at 1.2 nm for the shear simulations.

As previously discussed, ionic clusters are formed in PSS melts with both Na^+ and Mg^{2+} [1,2,5]. The ionic clusters, and their size distributions are depicted in Fig. 1 for 5% sulfonation level. We have defined a cluster by SO_3^- groups that are within 6 Å of each other. For 5% and 10% sulfonation, all of the clusters are finite in size and do not percolate across the sample. A close look at the cluster

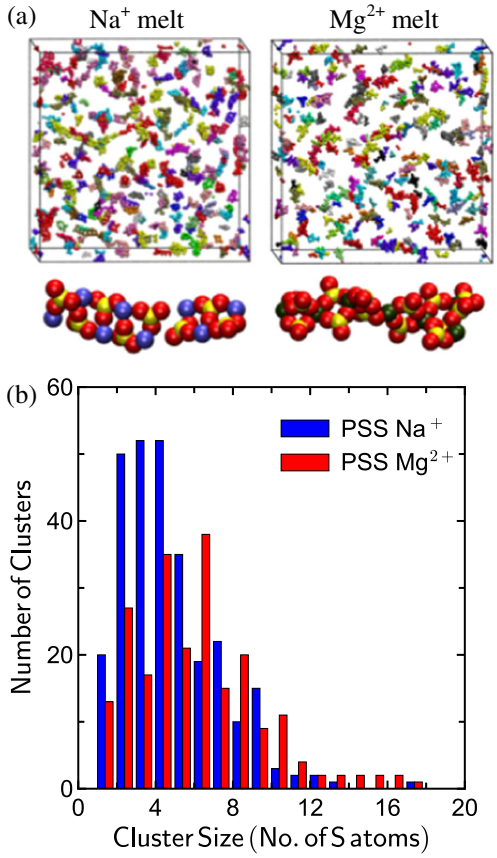

FIG. 1. (a) Representative clusters and (b) cluster distribution for 5% sulfonated polystyrene melts with Na^+ and Mg^{2+} counterions. PS chains in (a) are not shown for clarity. S (yellow), O (red), Na^+ (blue), and Mg^{2+} (green).

morphology of both melts in Fig. 1(a) show that in PSS/Na^+ melts many of the clusters are highly ordered, with ladderlike structure, whereas in PSS/Mg^{2+} while the clusters are elongated, they are more disordered. The cluster size distributions for both melts are presented in Fig. 1(b) are both very broad. The average cluster size in PSS/Na^+ melts is 4.1 sulfonation groups with cluster size that varies from 1 to 17 sulfonated groups, where the majority of clusters consist of 2 to 5 SO_3^- groups. The cluster distribution in the PSS/Mg^{2+} melts exhibits a similar size distribution with an average cluster size of 5.2 SO_3^- groups. The charge-neutral clusters with an even number of SO_3^- groups are dominant and positively and negatively charged clusters with an odd number SO_3^- groups appear to be less favored. The clusters in PSS/Mg^{2+} melts are more disordered and varied in morphology. Each Mg^{2+} ion is shared by 4 or more SO_3^- groups whereas in PSS/Na^+ melts, the counterion is shared by 2–3 SO_3^- groups. This new molecular insight distinguishes ordered and disordered clusters arising from the packing of ions with different charges.

Further insight into the clusters' structure was obtained from the static structure factor $S(q)$ for both melts. Ionic

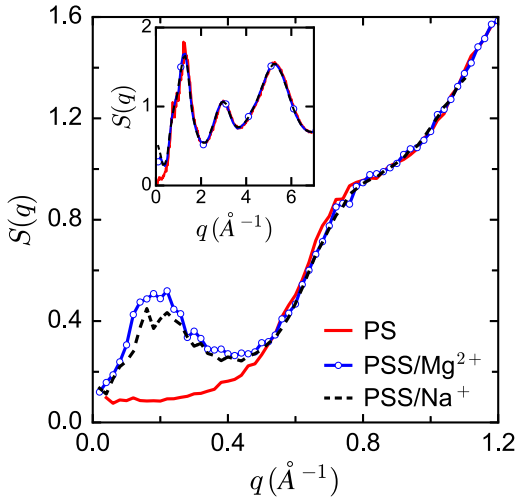

FIG. 2. $S(q)$ vs q for polystyrene and 5% sulfonated polystyrene with Na^+ and Mg^{2+} counterions. Inset shows the $S(q)$ for the full q range.

clustering was initially detected by scattering experiments and microscopy techniques [5,12–14,33,34]. $S(q)$ calculated from MD simulations were found to be in close agreement with the experimental ones [18]. The static structure factor is given by $S(q) = |\sum_i b_i e^{iq_i r_i}|^2 / \sum_i b_i^2$, where b_i, q_i, and r_i are the scattering length, momentum transfer vector, and position vector of atom i, respectively [35]. The results for polystyrene and for the two PSS melts are presented in Fig. 2. The patterns at high q values are identical for all polymers and the features correspond to intramolecular distances as shown in the inset. The ionic clusters signature is expressed as a broad peak centered around $q = 0.2$ Å^{-1}, presented in the main panel, which corresponds to an average cluster distance of ~30 Å. The $S(q)$ for polystyrene does not exhibit any features at the low q range as expected for a polymer without any ionic groups. These patterns are similar to those measured experimentally by Zhou *et al.* [5] for both PSS/Na^+ and PSS/Mg^{2+}. They observed a broad peak centered ~0.15 Å^{-1} for a similar range of sulfonation fractions at room temperature. The simulations point to smaller dimensions than the experimental data. The difference is attributed to slightly better packing of the chains obtained in atomistic simulation as a result of higher temperatures. Further, in contrast to the experiments where PSS absorbs water at ambient conditions, the simulation melts are water free. The signature of the ionic domains provides one important length scale associated with the confinement of the motion of the PSS molecules.

The dynamics of PSS was explored by calculating $S(q,t)$ [36,37]. Similar to Weiss and co-workers [14,16], who demonstrated that a small fraction of ionizable groups on polystyrene below its entanglement length results in constrained dynamics, our recent MD studies [10] have shown that the diffusion constant decreases from 1.7×10^{-8} cm^2/s

for 0 to 4.0×10^{-9} cm^2/s for 5% and 6.2×10^{-10} cm^2/s for 10% sulfonation in PSS/Na^+ melts. Here we first studied the center of mass diffusion for both melts; however, we did not detect any differences within the times we were able to access. We then probed segmental motion following the dynamic structure factor at different length scales. $S(q,t)$ for PSS melts with Na^+ and Mg^{2+} as counterions for different q values are shown in Fig. 3. On the length scales of the ionic domains reflected in $S(q)$ for PSS, i.e., q in the range of 0.1–0.5 Å^{-1}, the overall relaxation time surprisingly does not decrease monotonically with decreasing q as expected of diffusion of nonionic polymers in melts. Instead, $S(q,t)$ decays the slowest for $q = 0.2$ Å^{-1}, which corresponds to the ionic cluster signature in $S(q)$. This slow relaxation for $q \sim 0.2$ Å^{-1} is a result of quenching of the local motion on the length scale of the ionic clusters.

$S(q,t)$ differs in its decay from a single exponential that characterizes simple diffusion. It was analyzed in terms of a sum of two exponentials $S(q,t) = A_1 e^{-\Gamma_1 t} + A_2 e^{-\Gamma_2 t}$, where A_1 and A_2 are constants and Γ_1 and Γ_2 are effective diffusion coefficients (by definition $\Gamma_1 < \Gamma_2$). The fits are shown in Fig. 3 for Na^+ and Mg^{2+} PSS melts and their respective effective diffusion coefficients are shown in the inset. The slowest relaxation times $\sim 1/\Gamma_1$ decrease monotonically with increasing q. This q dependence shows that the slower decay in q around the low q peak in $S(q)$ is thus not due to a decrease in the long time effective diffusion constant (Γ_1) but is a consequence of reduction in the amplitude A_2 of the fast component (Γ_2) for $q \sim 0.2$ Å^{-1}. This is consistent with the ionic clusters acting as physical cross-linkers and inhibiting relaxation of the chains locally. Comparing the effective diffusion for PSS melts of both counterions shows that the slow component of the diffusion is similar for both melts; however, the faster component Γ_2 is larger for the Mg^{2+} melts than for the Na^+ ones. These differences could be attributed to disruption of packing of the chains around the magnesium clusters, which are more disordered, resulting in slightly less confined PS chains. These measurements of $S(q,t)$, coupling time, and length scales have provided a direct observation of the impact of clustering on dynamics that has been long postulated by rationalizing numerous experimental results.

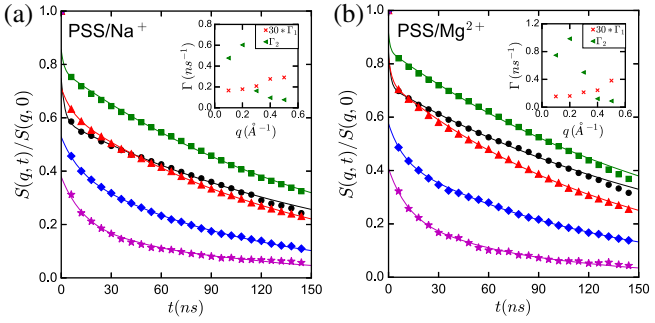

FIG. 3. $S(q,t)/S(q,0)$ vs time for various q values (symbols) and double exponential fit (solid line) to the data and gamma value with q in the inset for 5% sulfonated polystyrene with (a) Na^+ and (b) Mg^{2+} counterions. $S(q,t)/S(q,0)$ is plotted for q values of 0.1, 0.2, 0.3, 0.4, and 0.5 Å^{-1} represented by (circle, square, triangle, diamond and star), respectively.

To probe the macroscopic dynamics we measured the stress and calculated the shear viscosity of the sulfonated melts at 600 K as a function of strain rates. While for PS melt at both 500 and 600 K the viscosity has reached the shear rate independent plateau, the 5% and 10% PSS melts remain in the shear thinning regime for the computationally accessible lowest shear rate of 10^7/s. Over the entire range of shear rates studied, the shear viscosity of the 5% Mg^{2+} PSS melt is higher than that of the Na^+ PSS one, as demonstrated in the inset of Fig. 4. At the lowest shear rate accessible (10^7/s) the Na^+ PSS melt is beginning to cross over to the shear-rate-independent regime while PSS/Mg^{2+} melt is still in the shear-thinning regime.

The average radius of gyration of chains as a function of shear rate is shown in Fig. 5(a) for 5% sulfonation. For comparison, the mean squared radius of gyration is $\langle R_g^2 \rangle^{1/2} = 18.5$ Å for PSS/Na^+ and 19.0 Å for PSS/Mg^{2+}. As the melt is sheared, chains extend in the shear direction resulting in some clusters breaking up and forming new clusters. While the average cluster size increases with decreasing shear rates for both Mg^{2+} and Na^+, as shown in Fig. 5(b), the average cluster size is always larger for Mg^{2+}. This increase in the size of the long-lived ionic clusters for Mg^{2+} compared to Na^+ is consistent with the difference in the shear viscosity for the melts of the two counterions. The effect of shear strain on the ionic clusters is illustrated in Fig. 6, where t = 0 is the time when the shear is applied. With increasing strain, the chains opened up as evident from the increase in radius of gyration.

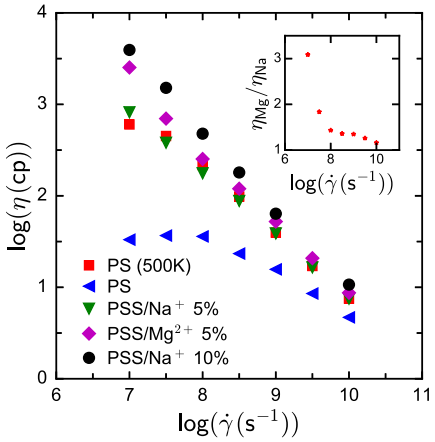

FIG. 4. Shear viscosity as a function of shear strain rate at 600 K for the indicated systems. The inset corresponds to the ratio of viscosities of PSS melts with Mg^{2+} and Na^+ counterions as a function of strain rate.

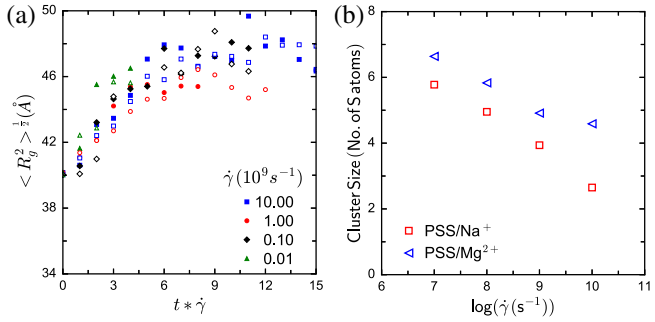

FIG. 5. (a) Radius of gyration as a function of shear cycles at indicated shear rates for 5% sulfonated polystyrene with Na^+ (open symbols) or Mg^{2+} (filled symbols) counterions. (b) Average cluster size with the shear rate.

With the chain opening up, clusters could break, grow, or rearrange depending on how ionic groups are distributed on the chain. A representative of a cluster rearranging in PSS/Na^+ melt is shown in Fig. 6(a). Here, a distorted cluster transforms into a ladderlike cluster with shear resulting in increase in the number of ordered ladderlike clusters in the melt. The cluster itself didn't break up due to the opening of the chains because the random ionic groups on different chains are involved. Because of the random distribution of the sulfonate groups on the polystyrene chain and given the small sulfonation fraction, there can be chains where sulfonate groups are distributed relatively evenly. When such chains stretch, ionic clusters may break up followed by rearrangements afterwards. A representative of this type of rearrangement is shown in Fig. 6(b) for PSS/Mg^{2+} melt, where there are three ionic clusters at the start of shearing which break and rearrange to give one large ionic cluster and a couple of smaller ionic groups as the aftermath of chain opening.

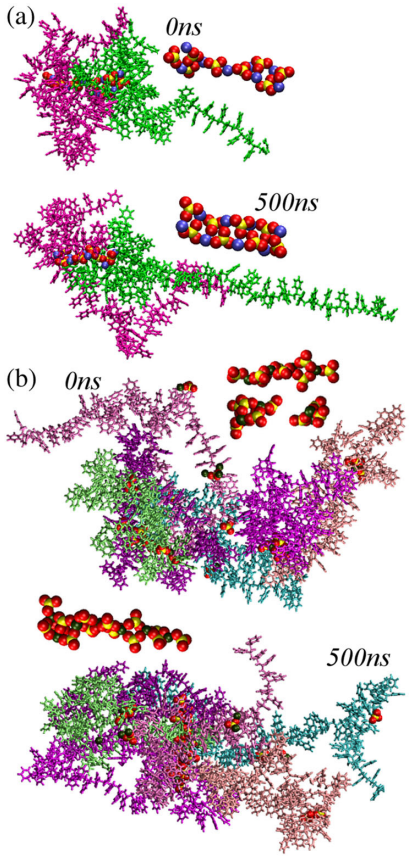

FIG. 6. Representative ionic cluster and chains with time at shear rate of 10^7 s^{-1} for 5% randomly sulfonated polystyrene with (a) Na^+ and (b) Mg^{2+} counterions.

In summary, accessing long simulation times, this study provides a fundamental molecular understanding that underlines the dynamics in ionic polymers. The structure, cluster size, and morphology of PSS melts with Na^+ and Mg^{2+} counterions were determined and correlated with chain dynamics, attained through measurements of $S(q,t)$ and shear viscosity, spanning multi time and length scales of motion. We find that PSS/Na^+ melts consist of well-defined ladderlike clusters and in PSS/Mg^{2+} more disorder clusters are formed. Although changing the counterion from Na^+ to Mg^{2+} did not have significant effect on the center of mass dynamics, on the time scales we were able to access, $S(q,t)$ revealed for the first time the correlation between the dimensions of the ionic clusters and the dynamics of the chains surrounding them. Upon applying of steady state shear, the viscosity of PSS/Mg^{2+} melt is much higher than that of PSS/Na^+ melt, which correlates directly with the larger cluster size of the Mg^{2+} melts. Overall, these observations through computational studies provided a new fundamental direct molecular insight into a long-lasting challenge in ionomers with an immense technological impact.

We gratefully acknowledge financial support from DOE Grant No. DE-SC007908 at Clemson University. We acknowledge computational resources at the National Energy Research Scientific Computing Center, which is supported by the Office of Science of the U.S. Department of Energy, under Contract No. DE-AC02-05CH11231 and Clemson Computing and Information Technology. This work was performed, in part, at the Center for Integrated Nanotechnologies, a U.S. Department of Energy and Office of Basic Energy Sciences user facility. Sandia National Laboratories is a multiprogram laboratory managed and operated by Sandia Corporation, a wholly owned subsidiary of Lockheed Martin Corporation, for the U.S. Department of Energy's National Nuclear Security Administration under Contract No. DE-AC04-94AL85000.

[1] A. Eisenberg and J.-S. Kim, *Introduction to Ionomers* (Wiley, New York, 1998).
[2] B. P. Grady, Polym. Eng. Sci. **48**, 1029 (2008).
[3] L. Zhang, N. R. Brostowitz, K. A. Cavicchi, and R. A. Weiss, Macromol. React. Eng. **8**, 81 (2014).

[4] D. G. Peiffer, R. A. Weiss, and R. D. Lundberg, J. Polym. Sci., Part B: Polym. Phys. **20**, 1503 (1982).
[5] N. C. Zhou, D. C. Chan, and K. I. Winey, Macromolecules **41**, 6134 (2008).
[6] B. Hird and A. Eisenberg, J. Polym. Sci., Part B: Polym. Phys. **28**, 1665 (1990).
[7] S. H. Kim and J. S. Kim, Macromolecules **36**, 2382 (2003).
[8] Q. Wu and R. A. Weiss, J. Polym. Sci., Part B: Polym. Phys. **42**, 3628 (2004).
[9] Q. Wu and R. A. Weiss, Polymer **48**, 7558 (2007).
[10] A. Agrawal, D. Perahia, and G. S. Grest, Phys. Rev. E **92**, 022601 (2015).
[11] B. Dreyfus, Macromolecules **18**, 284 (1985).
[12] B. P. Kirkmeyer, R. A. Weiss, and K. I. Winey, J. Polym. Sci., Part B: Polym. Phys. **39**, 477 (2001).
[13] A. M. Castagna, W. Wang, K. I. Winey, and J. Runt, Macromolecules **44**, 5420 (2011).
[14] R. A. Weiss and H. Zhao, J. Rheol. **53**, 191 (2009).
[15] G. H. Ling, Y. Wang, and R. A. Weiss, Macromolecules **45**, 481 (2012).
[16] X. Qiao and R. A. Weiss, Macromolecules **46**, 2417 (2013).
[17] D. S. Bolintineanu, M. J. Stevens, and A. L. Frischknecht, Macromolecules **46**, 5381 (2013).
[18] C. F. Buitrago, D. S. Bolintineanu, M. E. Seitz, K. L. Opper, K. B. Wagener, M. J. Stevens, A. L. Frischknecht, and K. I. Winey, Macromolecules **48**, 1210 (2015).
[19] J.-M. Y. Carrillo and A. V. Dobrynin, J. Phys. Chem. B **114**, 9391 (2010).
[20] S. Park, X. Zhu, and A. Yethiraj, J. Phys. Chem. B **116**, 4319 (2012).
[21] L. M. Hall, M. J. Stevens, and A. L. Frischknecht, Phys. Rev. Lett. **106**, 127801 (2011).
[22] W. L. Jorgensen, J. D. Madura, and C. J. Swenson, J. Am. Chem. Soc. **106**, 6638 (1984).
[23] W. L. Jorgensen, D. S. Maxwell, and J. Tirado-Rives, J. Am. Chem. Soc. **118**, 11225 (1996).
[24] X. He, O. Guvench, A. D. J. Mackerell, and M. L. Klein, J. Phys. Chem. B **114**, 9787 (2010).
[25] W. R. Cannon, B. M. Pettitt, and A. A. McCammon, J. Phys. Chem. **98**, 6225 (1994).
[26] J. Chandrasekhar, D. C. Spellmeyer, and W. L. Jorgensen, J. Am. Chem. Soc. **106**, 903 (1984).
[27] R. E. Isele-Holder, W. Mitchell, and A. E. Ismail, J. Chem. Phys. **137**, 174107 (2012).
[28] S. J. Plimpton, Comparative physiology **117**, 1 (1995).
[29] D. Evans and G. P. Morris, Comput. Phys. Rep. **1**, 297 (1984).
[30] J. W. Rudisill and P. T. Cummings, Rheol. Acta **30**, 33 (1991).
[31] D. J. Evans and G. P. Morriss, *Statistical Mechanics of Nonequilibrium Liquids* (Academic, New York 1990).
[32] M. E. Tuckerman, C. J. Mundy, S. Balasubramanian, and M. L. Klein, J. Chem. Phys. **106**, 5615 (1997).
[33] Y. S. Ding, S. R. Hubbard, K. O. Hodgson, R. A. Register, and S. L. Cooper, Macromolecules **21**, 1698 (1988).
[34] D. J. Yarusso and S. L. Cooper, Macromolecules **16**, 1871 (1983).
[35] C. M. Sorensen, Aerosol Sci. Technol. **35**, 648 (2001).
[36] B. Nystrom, J. Roots, J. S. Higgins, D. G. Peiffer, F. Mezei, and B. Sarkissian, J. Polym. Sci., Part C: Polym. Lett. **24**, 273 (1986).
[37] T. Kanaya, K. Kaji, R. Kitamaru, J. S. Higgins, and B. Farago, Macromolecules **22**, 1356 (1989).